

New shell model calculations for ^{40}Ar based on recent g -factor and lifetime measurements

K.-H. Speidel and S. Schielke

Helmholtz-Institut für Strahlen-und Kernphysik, Universität Bonn, Nussallee 14-16, D-53115, Germany

J. Leske, N. Pietralla, T. Ahn, and A. Costin

Institut für Kernphysik, TU Darmstadt, Schlossgartenstrasse 9, D-64289, Germany

O. Zell

Institut für Kernphysik, Universität zu Köln, Zùlpicher Str. 77, D-50937 Köln, Germany

J. Gerber

Institut de Recherches Subatomiques, F-67037 Strasbourg, France

P. Maier-Komor

Physik-Department, Technische Universität München, James-Franck-Str., D-85748 Garching, Germany

S. J. Q. Robinson

Physics Department, Millsaps College, Jackson, Mississippi 39210, USA

A. Escuderos, Y. Y. Sharon, and L. Zamick

Department of Physics and Astronomy, Rutgers University, Piscataway, New Jersey 08855, USA

(Received 3 March 2008; revised manuscript received 13 June 2008; published 23 July 2008)

We have redetermined the g factor and the lifetime of the 2_1^+ state in ^{40}Ar by applying the technique of α transfer from a carbon target to ^{36}S beams in inverse kinematics combined with transient magnetic fields. In addition, the lifetimes of the 4_1^+ and the 2_2^+ states in ^{40}Ar have been remeasured using the Doppler-shift-attenuation method (DSAM). Additional experimental details of the α -transfer measurements are provided. The results are discussed within the framework of new large-scale shell model calculations with both free and effective nucleon g factors.

DOI: [10.1103/PhysRevC.78.017304](https://doi.org/10.1103/PhysRevC.78.017304)

PACS number(s): 25.70.De, 21.10.Ky, 21.10.Dr, 27.40.+z

In a simple picture, the ^{40}Ar nucleus has two proton holes in the sd shell and two neutrons in the fp shell. With this structure the nucleus presents a good opportunity for studying the interesting effects, on the nuclear wave functions of its low-lying states, of the $N = 20$ shell closure, of the interplay between the neutrons and the proton holes, and of the possible $sd \rightarrow fp$ cross-shell excitations of protons and neutrons.

Recent measurements have been carried out for the g factors of the 2_1^+ states of all the stable even- A Ar isotopes [1,2]. A surprisingly continuous decrease of the experimental g -factor values from ^{36}Ar ($N = 18$) through ^{38}Ar ($N = 20$) to ^{40}Ar ($N = 22$) was observed. No obvious signatures were found in the Ar isotopes either for a rigid $N = 20$ neutron shell closure or for its significant breaking as is the case for the Ca isotopes [3,4]. This behavior was strikingly different from that of the neighboring sulfur isotopes [5]. There the $g(2_1^+)$ values exhibit a pronounced maximum at $N = 20$, clearly indicating, by the observed large value of $g(2_1^+)$ for ^{36}S , a dominant proton configuration for this state, and thus strongly supporting in that case the rigidity of the $N = 20$ neutron shell closure. Among the previous Ar data, the vanishingly small $g(2_1^+)$ value that was measured for ^{40}Ar , $g(2_1^+) = -0.02(4)$ [2], was quite surprising. Because the experiment was a difficult one, with an unexpectedly small, close to zero, result, this value therefore needed to be checked in another experiment. Since

this information is extremely important for the understanding of the structure of the Ar nuclei, we have remeasured it by employing an experimental technique that was different from the Coulomb excitation approach that was used exclusively in its two former measurements [2,6].

Some of the new ^{40}Ar data were already mentioned in our recent paper [5]. That article, however, concentrated on the ^{36}S results, obtained with Coulomb excitation, and on their theoretical interpretation. Here additional experimental details are provided about the α -transfer reaction utilized in that experiment to obtain the ^{40}Ar data. Several new deduced $B(E2)$ values are also included here. New large-scale shell model calculational results for ^{40}Ar are presented which agree well with the measured excitation energies, $B(E2)$ values, and $g(2_1^+)$ factor. In addition g factors are predicted for two other states. Our present calculational results are more extensive than in [2] and [5]. They also utilize a different shell model space and different effective nucleon g factors, and provide a perspective for isotones and isobars in this mass region.

The states of interest in ^{40}Ar were populated in the reaction $^{12}\text{C}(^{36}\text{S}, ^8\text{Be})^{40}\text{Ar}$ by bombarding a carbon target with a ^{36}S beam with an energy of 70 MeV. At this energy, close to the Coulomb barrier, states of predominantly low excitation energy and low spin are populated. This outcome is obviously a characteristic feature of the alpha-transfer mechanism, and is

clearly different from the evaporation scenario of a compound reaction. In the latter case, generally high angular momentum states are populated which decay through cascading γ rays (see also [7]).

Intense ^{36}S beams were obtained at the Cologne tandem accelerator by using highly enriched ^{36}S in the chemical compound FeS for the accelerator's ion source. The multi-layered target consisted of a 0.19 mg/cm^2 natural C layer on a 3.03 mg/cm^2 Gd layer which in turn was deposited on a 1.0 mg/cm^2 Ta foil backed by a 2.0 mg/cm^2 Cu layer. The nuclear reaction took place in the carbon layer, the Gd provided the transient field (TF) for spin precessions of the excited states, and the Cu served as a stopper for the ^{40}Ar nuclei in a hyperfine-interaction-free environment. In the measurements, the target was cooled to liquid nitrogen temperature and magnetized by an external field of 0.06 Tesla. In their collisions with the carbon nuclei, the ^{36}S projectiles were either Coulomb excited to high-lying states in ^{36}S or else transformed to ^{40}Ar via the α transfer mechanism. Both of these reactions were employed in the same experiment. The results for ^{36}S have been published recently [5] and we report here on the ^{40}Ar results.

The deexcitation γ rays were measured [with four $12.7\text{ cm} \times 12.7\text{ cm}$ NaI(Tl) scintillators and with a Ge detector of 40% relative efficiency] in coincidence with the two forward-emitted α particles from the decay of the recoiling ^8Be . The particle detector, a commercial Si counter of 300 mm^2 area and nominal $100\text{ }\mu\text{m}$ thickness, was placed at 0° relative to the beam axis. A Ta foil behind the target served as a beam stopper with its thickness adjusted to stop only the beam ions whereas the α particles could pass through to the Si detector. Figure 1 shows the low-lying level scheme of ^{40}Ar with the γ transitions relevant to the present work. Coincident particle spectra gated with all the γ rays are displayed in Fig. 2(a). The high energy peak is related to the two α particles associated with ^{40}Ar . Evidently, a clean separation of the α particle energies from the energies of the recoiling carbon

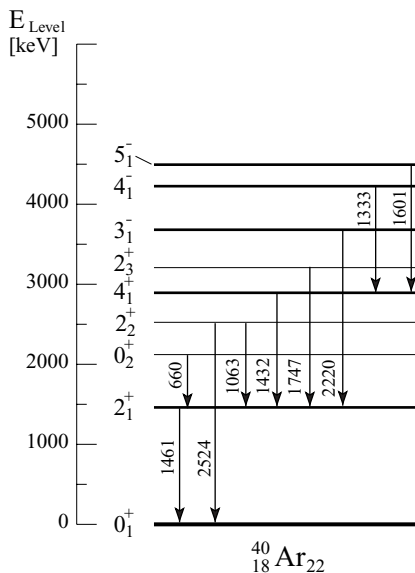


FIG. 1. Relevant level scheme and γ transitions in ^{40}Ar .

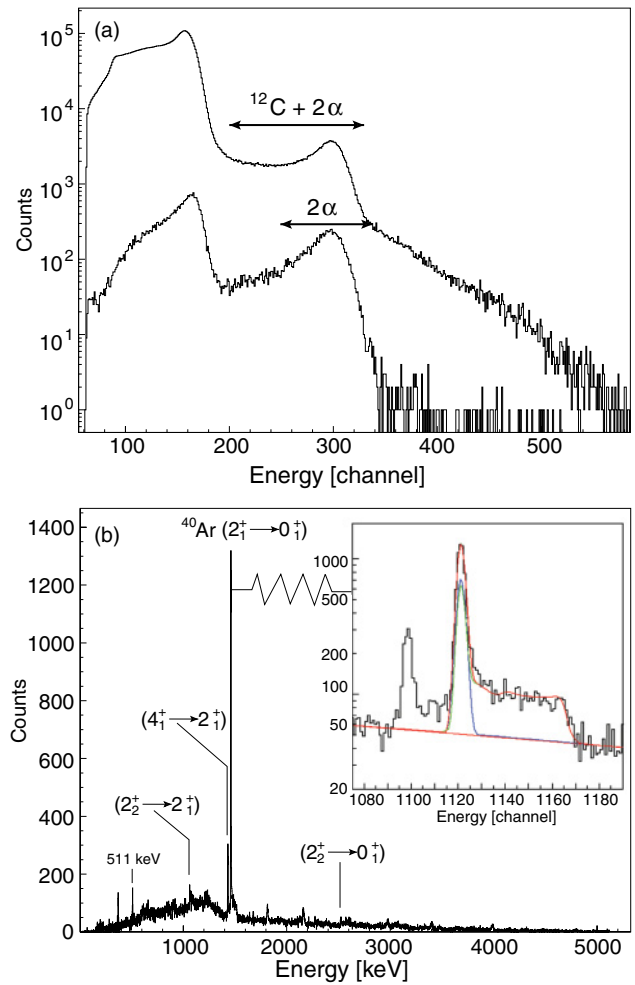


FIG. 2. (Color online) Coincidence spectra of (a) particles from a Si detector gated with all the γ rays (upper spectrum) or gated just with the ^{40}Ar ($2_1^+ \rightarrow 0_1^+$) γ line (lower spectrum), and of (b) γ rays from a Ge detector at 0° . The insert shows a DSAM fit to the lineshape of the ($2_1^+ \rightarrow 0_1^+$) 1461 keV transition in ^{40}Ar , including feeding from higher-lying states (see also text). The horizontal arrows in (a) denote the appropriate energy range in each case.

ions (corresponding to excited states in ^{36}S) was not feasible. Hence, in the γ -coincidence spectra, γ rays of both nuclei (^{40}Ar and ^{36}S) were present; however, there were no problems in separating the transitions of interest (see Fig. 2(b)).

Slopes of the particle- γ angular correlations and precessions were measured following the approach that was described in detail in [5,6]. For the ($2_1^+ \rightarrow 0_1^+$) transition an absolute slope value of $|S(65^\circ)| = 0.33(6)$ was obtained, which agrees well with the slopes found in previous α -transfer measurements (see also [1]). The relationship between the precession angle, Φ^{exp} , and the g factor of the state in question is given by [8]

$$\Phi^{\text{exp}} = g \frac{\mu_N}{\hbar} \int_{t_{\text{in}}}^{t_{\text{out}}} B_{\text{TF}}(v_{\text{ion}}(t)) e^{-\frac{t}{\tau}} dt. \quad (1)$$

Here, g is the g factor of the excited nuclear state, μ_N the nuclear magneton, and B_{TF} the transient field acting on the nucleus during the time interval ($t_{\text{out}} - t_{\text{in}}$) which the

TABLE I. Summary of the measured precession and calculated Φ^{lin}/g value. The newly determined lifetimes and deduced $B(E2)$ values, as well as the g factor of the 2_1^+ state, are compared with the literature values and with the results from large-scale shell model calculations (see text). For the calculated values the first result is in space I, the second in II.

E_f [MeV]		$I_i^\pi \rightarrow I_f^\pi$	$\tau(I_f^\pi)$ [ps]		Φ^{exp}	Φ^{lin}/g	$g(I_f^\pi)$			$B(E2) \uparrow [e^2 \text{fm}^4]$					
Exp.	Cal.		[11]	Exp. ^a	[mrad]	[mrad]	[2,6]	Exp. ^a	Cal(free)	Cal(eff.)	Exp. ^a	Cal.			
1.461	1.424	$(0_1^+ \rightarrow 2_1^+)$	1.62(6)	1.8(2)	-0.4(5)	22.0(9)	-0.02(4)	-0.02(3)	-0.197	-0.216	-0.068	-0.063	340(38)	252	239
							-0.1(1)								
2.892	2.742	$(2_1^+ \rightarrow 4_1^+)$	3.5(7)	2.6(4)					-0.354	-0.378	-0.269	-0.284	94(14)	70	63
2.524	2.865	$(0_1^+ \rightarrow 2_2^+)$	0.32(3)	0.7(1)					+0.120	-0.043	+0.290	+0.146	24(4)	41	18
		$(2_1^+ \rightarrow 2_2^+)$	-	0.6(2)									49(26)	25	22

^aPresent work.

ions spend in the Gd layer; the exponential factor accounts for the nuclear decay (with lifetime τ) in the target. The lifetimes were determined from measurements using the Doppler-shift-attenuation method (DSAM). The lineshapes of the respective γ lines were fitted to Monte Carlo simulations based on the reaction kinematics and the known stopping powers [9], using the computer code LINESHAPE [10]. Feeding from higher-lying states (4_1^+ and 2_2^+) was accounted for; it resulted in a contribution of $\sim 30\%$ to the stopped component of the $(2_1^+ \rightarrow 0_1^+)\gamma$ line of the $^{40}\text{Ar}(2_1^+)$ state. This is also the origin of the error for the 2_1^+ lifetime value quoted in Table I (see also Fig. 2(b)). In this specific case also background from the $(4_1^+ \rightarrow 2_1^+)\gamma$ line, underneath the $(2_1^+ \rightarrow 0_1^+)$ lineshape, was included in the global fit. The lifetime of the 2_2^+ state was determined from the analysis of two different γ lines (1063 keV and 2524 keV) emitted from the same state. In this case a large discrepancy was found from the 2_2^+ lifetime value in the literature [11].

The g factor of the $^{40}\text{Ar}(2_1^+)$ state was deduced from the measured precession angle by determining the effective TF strength in Eq. (1), using the empirical linear parametrization [8] and an attenuation factor $G = 0.96(4)$ for the magnetization of the Gd layer induced by the sulfur beam. The reliability of this approach was further confirmed by carrying out an additional calibration measurement, using the known g factor of the 2_1^+ state of a ^{48}Ti beam under similar experimental beam conditions on the same target (see also [5]). All the relevant ^{40}Ar data that were obtained in our experiment are summarized in Table I and are compared there with the literature values.

The present g factor result for the 2_1^+ state is in good agreement with the former values [2,6] and has the smallest uncertainty. The newly determined lifetime of this state is also consistent, within the errors, with the very precise value quoted in the literature [11]. On the other hand, the present data for the 2_1^+ lifetime, which tends to be larger than this literature value, is in excellent agreement with the adopted value, $\tau(2_1^+) = 1.89(21)$ ps, quoted by Raman *et al.* [12]. The same good agreement with the literature was obtained for the lifetime of the 4_1^+ state. In that case, the overall accuracy depended on the overlap of its lineshape with that of the $(2_1^+ \rightarrow 0_1^+)\gamma$ line which could not be completely disentangled (see also Fig. 2(b)). In contrast, a large discrepancy was found for the lifetime of the 2_2^+ state, with our lifetime being twice

that given in the literature [11]. In our case the final 2_2^+ lifetime value was determined from the analysis of two different γ lines (see Table I) with both resulting 2_2^+ lifetimes being consistent within their errors.

The experimental g -factor and the $B(E2)$ values of ^{40}Ar were compared in Table I with results of large-scale shell model calculations. These calculations were carried out with the computer code OXBASH [13] and employed the WBT effective interaction of Warburton and Brown [14]. Two different shell model spaces were utilized. Space I was $\pi(\text{full } sd)^{-2} \cdot \nu(\text{full } fp)^2$ (space E of [2]), with the calculations expanded also to the 4_1^+ and 2_2^+ states. Space II, with inert filled $d_{5/2}$ orbitals, was $\pi(d_{3/2}, s_{1/2})^{-2} \cdot \nu[(d_{3/2}, s_{1/2})^6(\text{full } fp)^2]$ with additional excitations of up to two nucleons (protons or neutrons) from $d_{5/2}s_{1/2}$ to the full fp shell permitted. The calculations used for the protons and neutrons, respectively, effective charges of $1.5e, 0.5e$, and free nucleon g factors $g_s = 5.586, g_l = 1$ and $g_s = -3.826, g_l = 0$. The $(\pi d_{3/2})^{-2}(\nu f_{7/2})^2$ configuration was found to be the dominant component (with over 70% of the probability) of both the 2_1^+ and 4_1^+ nuclear wave functions in the two spaces. Both spaces yield similar results in good agreement with the experimental values. The near congruence of the results, and the similarity of the corresponding wave functions, from both spaces explicitly indicates that in ^{40}Ar only a minor role is played by $sd \rightarrow fp$ shell nucleon core excitations (see also [2]). Such excitations, however, were required to explain the data for its $N = 22$ isotone ^{42}Ca [3,4].

In the following we compare the g -factor result for ^{40}Ar that we obtained with the measured $g(2_1^+)$ values of the other $N = 22$ isotones as the $Z = 20$ shell closure is approached, crossed, and left behind. The available data are $+0.13(5)$ for ^{38}S ($Z = 16$) [15], $-0.02(2)$ for ^{40}Ar ($Z = 18$) ([2] and present work), $+0.04(6)$ for ^{42}Ca ($Z = 20$) [3,4], and $+0.52(15)$ for ^{44}Ti ($Z = 22$) [16]. All these values are never large and negative despite the -0.547 Schmidt value for the $(f_{7/2})^2$ neutron configuration.

In a simple picture, below the $Z = 20$ shell closure, the $g(2_1^+)$'s are small with the positive sd shell proton g factors balancing the negative $f_{7/2}$ and $p_{3/2}$ neutron g factors. For ^{42}Ca , with the closed proton shell of $Z = 20$, the negative neutron g factors are balanced by the positive collective $g \approx Z/A$ values of the unexpectedly large excitations of the ^{40}Ca core. For the $N = Z$ ^{44}Ti nucleus, the isoscalar $g(2_1^+)$ factor is

well approximated by

$$g(2_1^+) = \frac{1}{2} \cdot [g(f_{7/2})_\pi^2 + g(f_{7/2})_v^2] \\ = \frac{1}{2} \cdot [(+1.655) + (-0.547)] = +0.544, \quad (2)$$

using the Schmidt values obtained utilizing the free nucleon spin and orbital g factors. The measured $g(2_1^+)$ value of ^{44}Ti is also consistent with the collective $g \sim Z/A = 0.5$ value. It should be noted that the same feature was observed for the $N = Z$ nuclei ^{32}S and ^{36}Ar (see [1,5]). Hence the possibility of substantial collective admixtures in the 2_1^+ wave function of ^{44}Ti cannot be excluded. This nucleus with the two protons and the two neutrons in the same orbitals, is the most collective of the above $N = 22$ isotones, with a measured $B(E2; 0_1^+ \rightarrow 2_1^+)$ value of $690(50) e^2 \text{ fm}^4$ [16], which is (2–3) times larger than the corresponding values in the other isotones: 235(30) for ^{38}S [15], 340(38) (present work) for ^{40}Ar and 330(20) for ^{42}Ca [3]. The approximate equality for the ^{40}Ar and ^{42}Ca values further indicates that the ^{40}Ca core is not totally rigid for ^{42}Ca .

It is interesting to compare the respective measured properties of the isobars ^{40}Ar and ^{40}S . The former was described as spherical [2] while the latter was depicted as being deformed [15,18]. However, some of their properties are almost identical: the $g(2_1^+)$ factors are very similar, $-0.02(2)$ (present work) vs $-0.01(6)$ [15,18]; also the $B(E2; 0_1^+ \rightarrow 2_1^+)$ values are very close, 340(38) (present work) vs $334(36)e^2 \text{ fm}^4$ [12]. But their $E(2_1^+)$ values differ substantially, 1.461 MeV vs 0.904 MeV, the latter smaller value suggesting greater collectivity for ^{40}S . For ^{40}Ar $E(4_1^+) = 2.892$ MeV, the ratio $E(4_1^+)/E(2_1^+) = 1.98$ and $Q(2_1^+) = +0.01(4)$ barns [19], very small and consistent with zero. On these grounds it would be highly valuable to measure the $E(4_1^+)$ and $Q(2_1^+)$ in ^{40}S ; these could help clarify the puzzle of why these two nuclei are so similar in some respects and yet quite different in other aspects.

It should be noted, as shown in Table I, that closer agreement with the ^{40}Ar $g(2_1^+) = -0.02(2)$ experimental value can be

obtained by using the effective neutron KBl g factors of Richter *et al.* [20] for $A = 41$, $g_s = -3.190$, $g_l = 0$, and the effective proton g factors for $A = 39$ of Brown and Wildenthal [21], $g_s = 4.660$, $g_l = 1.143$. In the two spaces I and II very similar values are then calculated for both the $g(2_1^+)$ and $g(4_1^+)$. Generally it is noted that all three g factors, in both spaces, are more positive when effective nucleon g factors are used.

In summary, using a different experimental technique, that of α transfer, we have remeasured the $g(2_1^+)$ factor in ^{40}Ar . Our work has reconfirmed that its value is very small and negative, in very good agreement with the earlier Coulomb-excitation results [2,6]. We have also redetermined the lifetimes of the 2_1^+ , 4_1^+ , and 2_2^+ states in ^{40}Ar . The first two lifetimes agree within error with those of the literature but our 2_2^+ lifetime value is twice as large as that of the literature. All our g factor and $B(E2)$ results are well explained by large-scale shell model calculations. The use of effective nucleon g factors significantly improves the agreement with the measured small $g(2_1^+)$ value (see also [2]).

The present results on ^{40}Ar demonstrate again that reactions involving α transfer from a carbon target to beams of stable nuclei are efficient nuclear spectroscopic tools. This approach is of particular interest for measurements on radioactive nuclei with a wide range of half-lives. It is a useful alternative to Coulomb excitation on secondary radioactive beams which were generally characterized by low intensities. Typical previous examples of very successful applications of α -transfer reactions were the measurements on radioactive ^{44}Ti [16] and ^{52}Ti [17] with half-lives of 60 yr and 1.7 min, respectively.

The authors are grateful to the operators of the accelerator. They acknowledge support by the BMBF, the Deutsche Forschungsgemeinschaft, and the Richard Stockton College of New Jersey.

-
- [1] K.-H. Speidel *et al.*, Phys. Lett. **B632**, 207 (2006).
 [2] E. A. Stefanova *et al.*, Phys. Rev. C **72**, 014309 (2005).
 [3] S. Schielke *et al.*, Phys. Lett. **B571**, 29 (2003).
 [4] K.-H. Speidel *et al.*, Phys. Rev. C **68**, 061302(R) (2003).
 [5] K.-H. Speidel *et al.*, Phys. Lett. **B659**, 101 (2008).
 [6] J. Cub *et al.*, Nucl. Phys. **A549**, 304 (1992).
 [7] O. Kenn *et al.*, Phys. Rev. C **65**, 034308 (2002).
 [8] K.-H. Speidel, O. Kenn, and F. Nowacki, Prog. Part. Nucl. Phys. **49**, 91 (2002).
 [9] F. J. Ziegler, J. H. Biersack, and U. Littmark, *The Stopping and Range of Ions in Solids* (Pergamon, Oxford, 1985), Vol. 1.
 [10] J. C. Wells and N. R. Johnson, computer code LINESHAPE, ORNL, 1994.

- [11] ENSDF, <http://www.nndc.bnl.gov/nndc/ensdf/>.
 [12] S. Raman *et al.*, At. Data Nucl. Data Tables **78**, 1 (2001).
 [13] A. Etchegoyen *et al.*, computer code OXBASH, MSU-NSCL, Report No. 524 (1985, unpublished).
 [14] E. K. Warburton and B. A. Brown, Phys. Rev. C **46**, 923 (1992).
 [15] A. D. Davies *et al.*, Phys. Rev. Lett. **96**, 112503 (2006).
 [16] S. Schielke *et al.*, Phys. Lett. **B567**, 153 (2003).
 [17] K.-H. Speidel *et al.*, Phys. Lett. **B633**, 219 (2006).
 [18] A. E. Stuchbery *et al.*, Phys. Rev. C **74**, 054307 (2006).
 [19] P. Raghavan, At. Data Nucl. Data Tables **42**, 189 (1989).
 [20] W. Richter *et al.*, Nucl. Phys. **A523**, 325 (1991).
 [21] B. A. Brown and B. H. Wildenthal, Nucl. Phys. **A474**, 290 (1987).